



**HAL**  
open science

## Modelling of the electrical admittance of a piezoceramic cube using Ultrasonic Resonance Spectroscopy

Oumar Diallo, Emmanuel Leclezio, Guy Feuillard

► **To cite this version:**

Oumar Diallo, Emmanuel Leclezio, Guy Feuillard. Modelling of the electrical admittance of a piezoceramic cube using Ultrasonic Resonance Spectroscopy. Acoustics 2012, Apr 2012, Nantes, France. hal-00810999

**HAL Id: hal-00810999**

**<https://hal.science/hal-00810999>**

Submitted on 23 Apr 2012

**HAL** is a multi-disciplinary open access archive for the deposit and dissemination of scientific research documents, whether they are published or not. The documents may come from teaching and research institutions in France or abroad, or from public or private research centers.

L'archive ouverte pluridisciplinaire **HAL**, est destinée au dépôt et à la diffusion de documents scientifiques de niveau recherche, publiés ou non, émanant des établissements d'enseignement et de recherche français ou étrangers, des laboratoires publics ou privés.



# ACOUSTICS 2012

## Modelling of the electrical admittance of a piezoceramic cube using Ultrasonic Resonance Spectroscopy

O. Diallo<sup>a</sup>, E. Leclézio<sup>b</sup> and G. Feuillard<sup>a</sup>

<sup>a</sup>Université de TOURS, Enivl Rue de la Chocolaterie, 41034 Blois, France

<sup>b</sup>Université Montpellier 2 - IES - UMR CNRS 5214, place Eugene Bataillon, cc 082, 34095

Montpellier, France

oumar.diallo@univ-tours.fr

Ultrasonic Resonance Spectroscopy allows the characterisation of piezoelectric materials thanks to the study of their mechanical and electrical resonances. In this context, the present work deals with the modelling of the electrical admittance of parallelepiped shaped piezoelectric samples. First, the natural mechanical and electrical resonant frequencies of a piezoelectric cube are calculated from the stationary points of the Lagrangian of the system. Then its electrical resonances are identified taking into account the short circuit electrical boundary conditions and the electrical admittance is determined as a function of frequency from calculations of the charge quantity on both electrodes of the cube. Measurements are carried out on a PMN-34.5PT ceramic cube. According to the properties determined by mechanical velocity measurements, the cube presents a first resonance around 125 kHz. Experimental admittance curves are compared with success to the electrical modelling of the cube vibrations.

## 1 Introduction

Several models of one-dimensional vibrations of a piezoelectric material can be found in the literature, such as Mason's and KLM, which can predict the electromechanical behaviour of a piezoelectric plate. These methods are not applicable to 3D specimens such as a cube. Until now, conventional techniques use several samples to identify the material parameters [1]. Recently, Delaunay *et al.* proposed an ultrasonic characterization method allowing the determination of these properties using a single sample. This method, referred to as Resonant Ultrasound Spectroscopy [2], examines the vibration modes of a piezoelectric cube and relates mechanical resonances measured by Laser interferometry to electromechanical properties. This method is here modified to obtain the electromechanical properties of a metallized sample from the study of its electrical admittance and optical measurements. At first, the eigenfrequencies of a piezoelectric cube with electrodes on two faces will be calculated. Secondly, its electrical admittance will be modelled. This admittance will be compared to the experimental results. Finally, the validity of the model will be discussed.

## 2 Eigenfrequencies of a piezoelectric cube

### 2.1 Calculation of the stationary points

The calculation of the stationary points of a system implies the minimization of its Lagrangian expression:

$$L = \iiint_V (E_c - E_{def} - E_p - E_e) dV \quad (1)$$

where  $E_c$  is the kinetic energy,  $E_{def}$  is the deformation energy,  $E_p$  is the potential energy and  $E_e$  is the electrostatic energy.

Here, a piezoelectric cube is considered, as shown in figure 1.

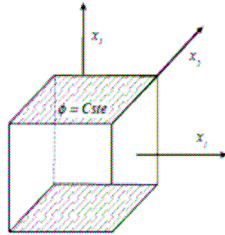


Figure 1: Piezoelectric parallelepiped with dimensions A, B and C (here A = B = C = 10 mm) and poled along  $x_3$ .

The origin of the axis is taken at the centre of the piezoelectric sample such as  $L_1=A/2$ ,  $L_2=B/2$  and  $L_3=C/2$

where A, B and C are the edges' lengths of the parallelepiped. There are two electrodes on the faces  $x_3=L_3$  and  $x_3=-L_3$ . The general Lagrangian can be expressed as [4, 5]

$$L = \iiint_V \frac{1}{2} (u_{i,j} C_{ijkl}^E u_{k,l} - \rho \omega^2 u_i u_i) dV + \iiint_V \frac{1}{2} (2\phi_{,m} e_{mkl} u_{k,l} - \phi_{,m} \epsilon_{mn}^S \phi_{,n}) dV - \sum_{S=1}^2 \iint_S N_m \phi (e_{mkl} u_{k,l} - \epsilon_{mn}^S \phi_{,n}) dS \quad (2)$$

The summation on indices runs from 1 to 3, corresponding to the three directions in the coordinate space.

To minimize the Lagrangian (and hence find the equilibrium configuration of the system), the Rayleigh-Ritz method is used. The displacements and electrical potential are then expressed as a linear combination of the trial functions:

$$\vec{u}_i = \sum_{p=1}^N a_p \vec{\psi}_p \quad \text{and} \quad \phi = \sum_{r=1}^M b_r \varphi_r \quad (3)$$

The  $(\psi_p)_{p=1\dots N}$  and  $(\varphi_r)_{r=1\dots M}$  functions are chosen to be orthonormal [2].

If these relations are injected in equation (2) the Lagrangian becomes:

$$L = \frac{1}{2} \left[ \sum_p \sum_{p'} a_p a_{p'} (\Gamma_{pp'} - \rho \omega^2 \delta_{pp'}) \right] + \sum_p \sum_r a_p b_r (\Omega_{pr} - A_{pr}) - \frac{1}{2} \left[ \sum_r \sum_{r'} a_r a_{r'} (\Lambda_{rr'} - B_{rr'}) \right] \quad (4)$$

where,

$$\begin{aligned} \Gamma_{pp'} &= \iiint_V \psi_{pi,j} C_{ijkl}^E \psi_{p'k,l} dV \\ \Omega_{pr} &= \iiint_V \varphi_{r,m} e_{mkl} \psi_{pk,l} dV \\ \Lambda_{rr'} &= \iiint_V \varphi_{r,m} \epsilon_{mn}^S \varphi_{r',n} dV \\ A_{pr} &= \sum_{S=1}^2 \iint_S \varphi_r N_m e_{mkl} \psi_{pk,l} dS \\ B_{rr'} &= \sum_{S=1}^2 \iint_S \varphi_r N_m \epsilon_{mn}^S \varphi_{r',n} dS \end{aligned} \quad (5)$$

with

$$\psi_{pi,j} = \frac{1}{2} \left( \frac{\partial \psi_{pi}}{\partial x_j} + \frac{\partial \psi_{pj}}{\partial x_i} \right) \quad \text{and} \quad \varphi_{r,m} = \frac{\partial \varphi_r}{\partial x_m} \quad (6)$$

$\Gamma$ ,  $\Omega$  and  $\Lambda$  are the elastic, piezoelectric and dielectric interaction matrices respectively.  $A_{pr}$  and  $B_{r'}$  are the contributions of the work of the electrostatic forces. Coefficients  $a_p$  and  $b_r$  are obtained by calculating the stationary points of the Lagrangian (*i.e.*  $\partial L=0$ ). This yields the following eigenvalue system:

$$\begin{aligned} (\Gamma + (\Omega - A)(\Lambda - 2B)^{-1}(\Omega - A)^t) a &= \rho \omega^2 a, \\ b &= (\Lambda - 2B)^{-1}(\Omega - A)^t a. \end{aligned} \quad (7)$$

The eigenvectors of this equation system give the coefficients of the expansion of the displacements and electrical functions of the sample in terms of the basis functions. The eigenvalues are linked to the resonance frequencies.

## 2.2 Basis trial functions

To apply this technique, one should chose basis functions for the particle displacements and electrical potential that match the configuration of our system. The displacement trial functions must satisfy:

$$\delta_{pp'} = \begin{cases} 1 & \text{if } p = p' \\ 0 & \text{otherwise} \end{cases} \quad (8)$$

The electric potential trial functions must correspond to the short circuit or zero potential boundary condition on the electrodes. Although this is not a necessary condition, it increases the computation convergence and simplifies the calculation of the interaction matrices. The chosen basis functions of displacement and electrical potential are respectively:

$$\psi_p = \frac{1}{\sqrt{L_1 L_2 L_3}} P_\lambda \left( \frac{x_1}{L_1} \right) P_\mu \left( \frac{x_2}{L_2} \right) P_\nu \left( \frac{x_3}{L_3} \right) \vec{e}_i \quad (9)$$

$$\varphi_r = \frac{1}{\sqrt{L_1 L_2 L_3}} P_\xi \left( \frac{x_1}{L_1} \right) P_\zeta \left( \frac{x_2}{L_2} \right) f_\eta$$

with  $f_\eta = \sin \left( (\eta + 1) \left( 1 + \frac{x_3}{L_3} \right) \right) P_\eta \left( \frac{x_3}{L_3} \right)$  where the  $p^{\text{th}}$

and  $r^{\text{th}}$  basic functions  $\psi_p$  and  $\varphi_r$  are defined by the triplets,  $(\lambda, \mu, \nu)$  and  $(\xi, \zeta, \eta)$ , respectively.  $P_\alpha(x)$  is the normalized Legendre function of order  $\alpha$  and  $e_i$  is the unit displacement vector in  $x_i$  direction,  $\frac{1}{\sqrt{L_1 L_2 L_3}}$  is a normalization term [2, 4, 5].

## 2.3 Simulation results

Table 1 shows the first thirty ordered resonance frequencies of a  $10 \times 10 \times 10 \text{ mm}^3$  PMN-34.5PT piezoelectric cube calculated using the previous model. The elastic, piezoelectric and dielectric constants were taken from [2]. They are  $C_{11}=174.7$ ,  $C_{12}=116.6$ ,  $C_{13}=119.3$ ,  $C_{33}=154.8$ ,  $C_{44}=26.7$ ,  $C_{66}=29$  in GPa;  $e_{15}=17,1$ ,  $e_{31}=-6.92$ ,  $e_{33}=27.3$  in C/m<sup>2</sup>;  $\epsilon_1=21.0105$ ,  $\epsilon_3=25.0125$  in pF/m.

The six first resonance frequencies correspond to the static modes (three rotations and three translations). In a free system all these six frequencies are null but here the boundary conditions in direction  $x_3$  are different. Some

frequencies are degenerated. They represent the same mode with a rotation of  $90^\circ$  around the polarisation axis  $x_3$ . These eigen-frequencies correspond to both mechanical and electrical resonances. Next, one needs to determine which frequencies among these are piezoelectrically coupled.

Table 1: The computed eigenfrequencies

| Frequencies in Hz |        |        |        |        |        |
|-------------------|--------|--------|--------|--------|--------|
| 0                 | 0      | 0      | 0      | 23282  | 23282  |
| 86616             | 87522  | 103377 | 103377 | 113423 | 116738 |
| 120113            | 122297 | 124643 | 124643 | 132688 | 134243 |
| 141163            | 141163 | 153051 | 156508 | 156508 | 156561 |
| 159303            | 160884 | 160884 | 165250 | 165250 | 166979 |

## 2.4 Calculation of electrical admittance

To compute the electrical admittance,  $Q_p$  is defined as the free charge on electrode  $p$ :

$$Q_p = \iint_S (e_{3kl} u_{k,l} - \epsilon_{3n}^S \phi_{,n}) dS \quad (10)$$

To calculate the admittance matrix formulas, it is necessary to express the current:

$$I = -j \omega \iint_S (N_3 D_3) dS \quad (11)$$

Differentiation of the current with the electric potential gives the electrical admittance matrix expressed as [4].

$$Y = j \omega C^S + j \omega \sum_i Q_i^2 / (\omega_i^2 - \omega^2) \quad (12)$$

where  $i$  is the number of the mode and  $C^S$  is the clamped capacitance given by:

$$C^S = 2 \epsilon_{33}^S L_1 L_2 / L_3. \quad (13)$$

## 2.5 Simulation of the electrical admittance:

In this paragraph, data from section 2.3 and the previously computed eigen-frequencies are used. To compute the admittance, the particle displacement and the electric potential are calculated. Figure 2 shows the modulus of the admittance obtained with this technique.

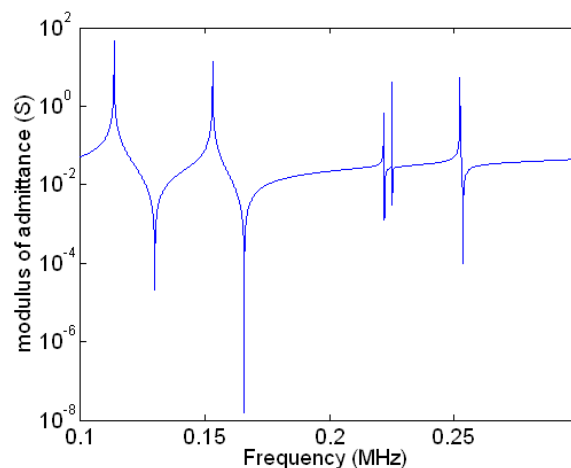


Fig. 2: Computed modulus of the electrical admittance of the PMN34.5PT cube.

There are five electrical resonances, meaning that in this domain only five modes are piezoelectrically coupled. Table 2 shows these sorted frequencies.

Table 2: Computed frequencies of piezoelectrically-coupled resonance modes

| Frequencies in Hz |        |        |        |        |
|-------------------|--------|--------|--------|--------|
| 113400            | 153100 | 221800 | 225300 | 252500 |

### 3 Experimental Results

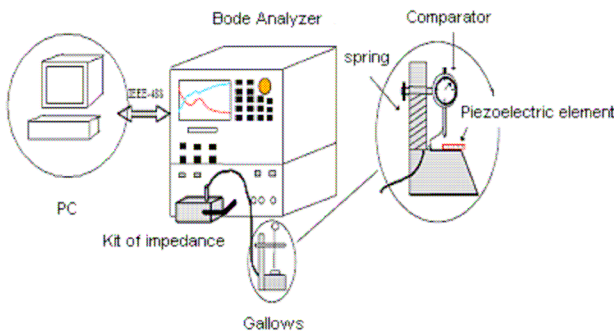


Fig. 3: Experimental set-up

The experimental set-up used to measure the admittance of the PMN34.5PT cube is presented in figure 3. Results are presented in figure 4.

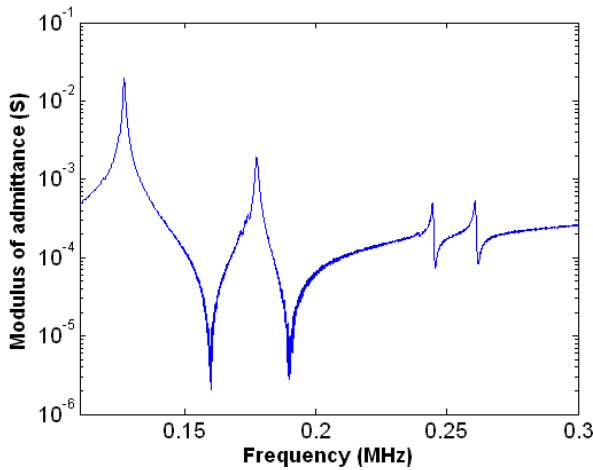


Fig. 4: Measured electrical admittance of PMN34.5PT cube

One can observe five resonances in the admittance curve, the frequencies of which are given in table 3.

Table 3: The measured frequencies of piezoelectrically coupled modes

| Electrical resonance frequencies in Hz |        |        |        |        |
|--|--------|--------|--------|--------|
| 126900                                 | 177500 | 239400 | 244600 | 260800 |

### 4 Comparisons and discussions

Theoretical and experimental resonance frequencies differ of approximately 10%. These discrepancies can result from the fact that the model does not take into account the viscoelastic behaviour of the material while the experimental resonances presented in figure 4 are clearly affected in amplitude and quality. A second reason can be that the constants used in the simulations do not exactly correspond to the electromechanical properties of our PMN34.5PT sample.

To test this hypothesis, let's evaluate the effect of a change of some functional properties on the admittance curves and its resonance frequencies. If the  $C_{13}$  constant is reduced by 5%, the curve of figure 5 is obtained and the new resonance frequencies are shown in table 4 reveal the high dependence of the resonance frequencies to the  $C_{13}$  characteristic

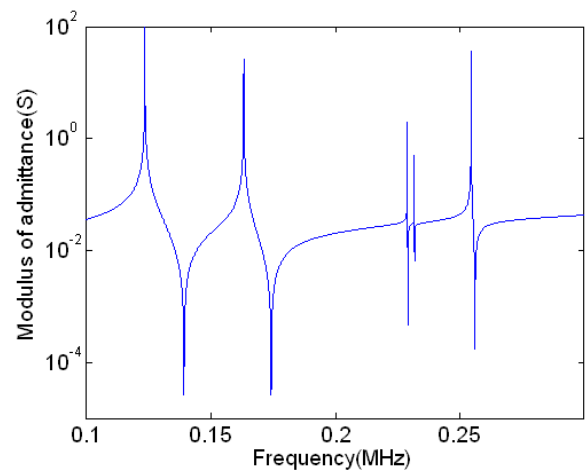


Fig. 5: Computed modulus of the electrical admittance of PMN34.5PT cube.

Like previously we have five frequencies piezoelectrically coupled.

Table 4: The computed frequencies of piezoelectrically coupled modes using the modified properties.

| Electric Resonance Frequencies in Hz |        |        |        |        |
|--------------------------------------|--------|--------|--------|--------|
| 123400                               | 163200 | 228900 | 231700 | 254600 |

A sensitivity study of the resonance frequencies to the input parameters is then performed. Table 5 shows the sensitivity to the elastics parameters of the resonance frequencies of piezoelectrically coupled mode.  $C_{13}$  is the coefficient with the biggest influence while  $C_{44}$  and  $C_{66}$  have no effect on the frequency of the first mode being a thickness mode. They also less influence the second mode than the others (see figure 6). These results indicate that a good precision on the input elastics parameters is required to allow a accurate representation of the resonance spectrum.

Table 5: Sensitivity to the elastic constants of the computed resonance frequencies of piezoelectrically coupled modes (in Hz/GPa)

| Mode | $C_{11}$ | $C_{33}$ | $C_{44}$ | $C_{66}$ | $C_{12}$ | $C_{13}$ |
|------|----------|----------|----------|----------|----------|----------|
| 1    | 458      | 891      | 0        | 0        | 377      | -1676    |
| 2    | 630      | 891      | 75       | 69       | 292      | -1693    |
| 3    | 550      | 672      | 974      | 483      | 206      | -1190    |
| 4    | 2851     | 556      | 1423     | 828      | -69      | -1073    |
| 5    | 904      | 168      | 300      | 1862     | -703     | -352     |

To increase the confidence in our model, let's verify if the theoretical and experimental modes are in accordance. For this, the deformation of the face  $x_3=L_3$  was measured using a Laser vibrometer (Polytech OFV-505). It allows the resonance frequencies to be detected and to identify the associated mode shapes. A voltage generator delivers an electrical excitation. It has a very large frequency bandwidth and the delivered electrical power is adjustable. The sample is set on a plastic holder and the electrical contact is ensured by a metallic strip fixed on a spring so that free mechanical boundary conditions at the surfaces of the cube are fulfilled [2]. The interferometer is positioned at 50 cm from the sample. The velocity decoder sensitivity is respectively 5 mm/s/V and 25 mm/s/V, depending on the cut-off frequency, respectively 250 kHz and 1,5 MHz. The measured signals are sent to a computer via a digital oscilloscope. Figure 6 shows the theoretical and experimental displacements associated to the piezoelectrically coupled modes.

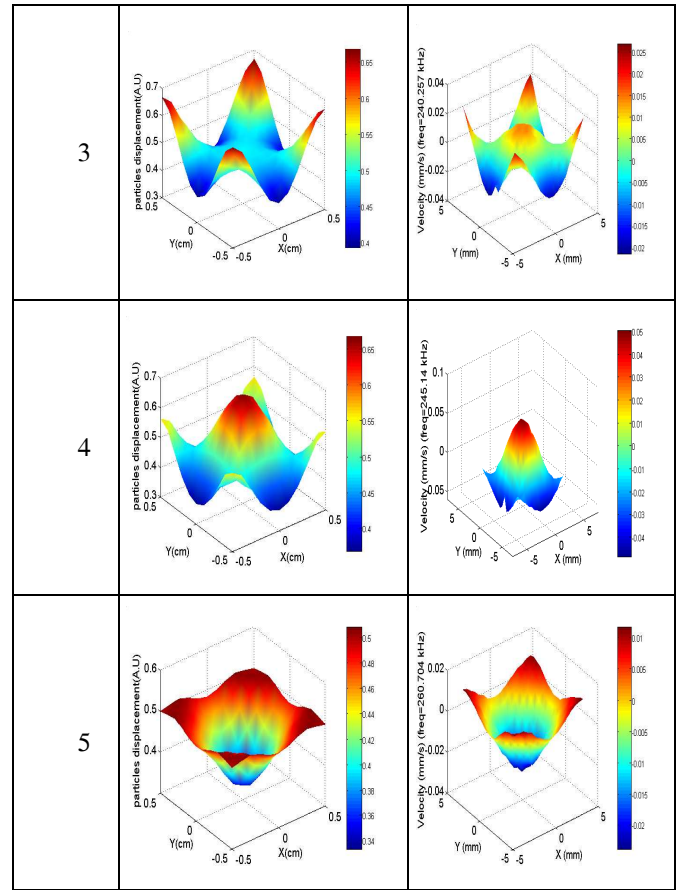
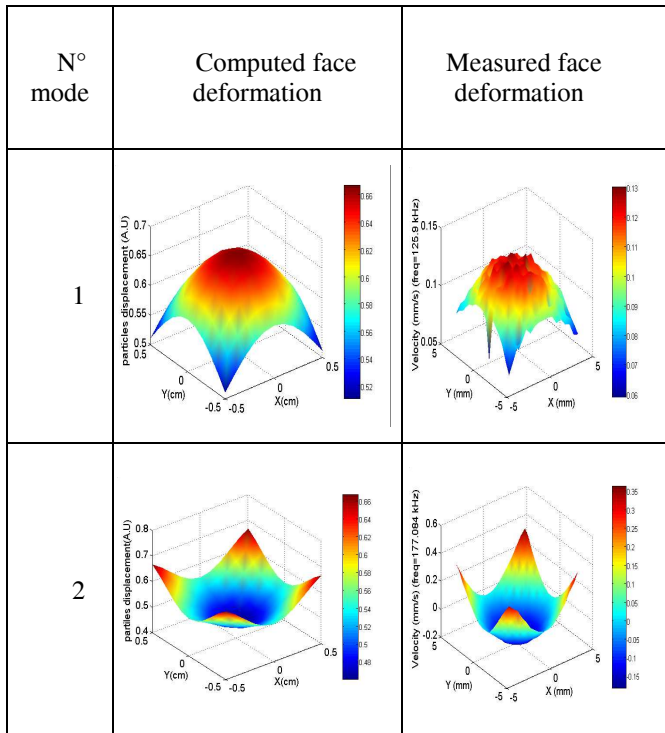


Fig. 6 : Computed and measured particle displacements of the five piezoelectrically coupled modes

The theoretical and experimental aspects of particle displacements are in accordance for all five modes, validating the model.



## 5 Conclusion

In this paper we have studied the eigen-vibration modes of piezoelectric cubes. We have calculated the electrical admittance of the cube and shown that electrical boundary conditions strongly influence the piezoelectrically coupled modes. In the frequency bandwidth of the study, there is a good agreement between the theoretical and experimental particle displacements at the surface of the studied cube. However, resonance frequencies are not located exactly at the expected values due to their strong sensitivity to the material electromechanical parameters. In further studies, we will introduce electrical and mechanical losses in order to compute the amplitude of the admittance and quantify their influence on the resonances. Then, thanks to a sensitivity study, the inverse problem will be solved to identify the properties of the material.

## References

- [1] "Publication and proposed revision of ANSI/IEEE Standard 176-1987 on piezoelectricity," IEEE Trans. Ultrason., Ferroelect., Freq. Contr. **43**, 717 (1996).
- [2] T. Delaunay et al., *Full tensorial characterization of PZN-12PT single crystal by Resonant Ultrasound Spectroscopy*, IEEE Trans. on UFFC control **55**, 476 (2008).
- [3] R. Holland et al., *Variational Evaluation of admittances of Multielectroded Three-Dimensional Piezoelectric Structures*, IEEE Trans. on Sonics and Ultrasonics, 119 (1968)
- [4] I. Ohno, *Free vibration of a rectangular parallelepiped crystal and its application to determination of elastic constants of orthorhombic crystals*, J. Phys. Earth, **24**,355(1976)
- [5] H. Demarest, *Cube-Resonance Method to Determine the Elastic Constants of Solids*, J. Acous. Soc. Am., **49**, 768 (1971)